Contrasting dynamic responses in vivo of the Bcl-x_L and Bim erythropoietic survival pathways

*Miroslav Koulnis,[1] *Ermelinda Porpiglia,[1] P. Alberto Porpiglia,[1] Ying Liu,[1] Kelly Hallstrom,[1] Daniel Hidalgo,[1] and Merav Socolovsky[1]

[1]Departments of Pediatrics and Cancer Biology, University of Massachusetts Medical School, Worcester, MA

Survival signaling by the erythropoietin (Epo) receptor (EpoR) is essential for erythropoiesis and for its acceleration in hypoxic stress. Several apparently redundant EpoR survival pathways were identified in vitro, raising the possibility of their functional specialization in vivo. Here we used mouse models of acute and chronic stress, including a hypoxic environment and β-thalassemia, to identify two markedly different response dynamics for two erythroblast survival pathways in vivo. Induction of the antiapoptotic protein Bcl-x_L is rapid but transient, while suppression of the proapoptotic protein Bim is slower but persistent. Similar to sensory adaptation, however, the Bcl-x_L pathway "resets," allowing it to respond afresh to acute stress superimposed on a chronic stress stimulus. Using "knock-in" mouse models expressing mutant EpoRs, we found that adaptation in the Bcl-x_L response occurs because of adaptation of its upstream regulator Stat5, both requiring the EpoR distal cytoplasmic domain. We conclude that survival pathways show previously unsuspected functional specialization for the acute and chronic phases of the stress response. Bcl-x_L induction provides a "stop-gap" in acute stress, until slower but permanent pathways are activated. Furthermore, pathologic elevation of Bcl-x_L may be the result of impaired adaptation, with implications for myeloproliferative disease mechanisms. (*Blood*. 2012;119(5): 1228-1239)

Introduction

Basal red cell production, as well as its acceleration by hypoxic stress,[1] requires the hormone Erythropoietin (Epo). Epo exerts its effect by activating its receptor, EpoR, on the surface of erythroid progenitors.[2] CFU-erythroid (CFU-e) progenitors and their immediate proerythroblast and basophilic erythroblast progeny are Epo dependent.[3] Until recently, the rarity of these cells within hematopoietic tissue confined their biochemical study to in vitro culture systems, where they were found to undergo apoptosis when deprived of Epo.[4] It was therefore suggested that Epo regulates erythropoietic rate through the number of erythroid progenitors it rescues from apoptosis.[4]

Recently, we[5] and others[6,7] made use of cell-surface markers to identify maturation-specific erythroblast subsets directly within freshly isolated mouse hematopoietic tissue,[5] including the Epo-responsive ProE (proerythroblasts, $CD71^{high}Ter119^{medium}$) and EryA (early basophilic erythroblasts, $CD71^{high}Ter119^{high}FSC^{high}$). This approach confirmed the central role of apoptosis in the erythropoietic stress response, showing that a substantial fraction of the early erythroblast compartment, particularly splenic ProE and EryA, undergo apoptosis in vivo in the normal basal state. Stress-induced high Epo levels suppress apoptosis and consequently promote early erythroblast expansion and an increase in erythropoietic rate.[5]

Although several EpoR-activated survival pathways have been identified,[8-12] relevance to erythropoiesis in vivo was documented for only a few, largely through gene "knockout" studies revealing abnormal basal or stress erythropoiesis.[8,13-16] Importantly, it is unknown how multiple survival pathways integrate in vivo to provide a coherent erythropoietic stress response, and whether the large number of survival pathways represents redundancy or functional specialization. The study of these pathways in vivo, now made possible with the advent of flow cytometric techniques,[5-7,17] may assist in answering this question.

We recently investigated the role of the death receptor Fas, and its ligand, FasL, which are coexpressed by early erythroblasts and suppressed by EpoR signaling in vivo.[5,18,19] We found that, in addition to regulating cell survival, this pathway stabilizes basal erythropoiesis and accelerates its response to stress.[19] Therefore, antiapoptotic pathways may have system-level functions that are not apparent from their antiapoptotic effects in culture. Here we set out to investigate two apoptotic regulators of the Bcl-2 protein family that are targeted by EpoR signaling, the antiapoptotic protein Bcl-x_L and the proapoptotic Bim protein. EpoR-activated Stat5 induces Bcl-x_L[8,20] synergistically with GATA1, a major survival pathway in erythroblasts.[21-23] Bcl-$x_L^{-/-}$ mice die in utero of anemia, and Bcl-$x_L^{-/-}$ ES cells fail to contribute to erythropoiesis in chimeric mice.[24] In a Stat5-deficient mouse,[25] reduced Bcl-x_L in early erythroblasts results in ineffective erythropoiesis and anemia.[13] Severe ineffective erythropoiesis in adult erythroblasts conditionally deleted for Bcl-x_L[15] is corrected if mice are also deleted for the proapoptotic proteins Bax and Bak,[26] suggesting that the requirement for Bcl-x_L in erythropoiesis is a result of its antiapoptotic effect. Furthermore, using conditional deletion for Bcl-x_L, it was found that it mediates over half the antiapoptotic effect of EpoR signaling in early erythroblasts.[27]

Submitted July 3, 2011; accepted October 21, 2011. Prepublished online as *Blood* First Edition paper, November 15, 2011; DOI 10.1182/blood-2011-07-365346.

*M.K. and E.P. contributed equally.

The online version of this article contains a data supplement.

The publication costs of this article were defrayed in part by page charge payment. Therefore, and solely to indicate this fact, this article is hereby marked "advertisement" in accordance with 18 USC section 1734.

Despite the clear role for Bcl-x_L in basal erythropoiesis, it is not known whether it is up-regulated by Epo during stress. Elevated erythroblast Bcl-x_L was implicated in polycythemia vera,[28,29] suggesting it has the potential to enhance erythroblast survival and erythropoiesis above the basal rate.[29]

We contrasted Bcl-x_L with Bim, a BH3-only proapoptotic Bcl-2 family protein.[30] Bim down-regulation is a key component of survival signaling by cytokines and oncoproteins in hematopoietic progenitors.[31,32] EpoR signaling in vitro was recently shown to decrease Bim mRNA[11,33] and enhance ERK-mediated degradation of the Bim protein.[33] Like Bcl-x_L, in addition to EpoR signaling, Bim is also regulated by GATA-1, via its transcriptional target LRF.[34] LRF$^{-/-}$ mice die in utero secondary to severe erythroblast apoptosis, partly rescued by Bim deletion.[34] Despite the clear role for Bim suppression in erythroblast survival, it is not known whether this pathway participates in the stress response.

Here we used intracellular multiparameter flow cytometry to measure Bcl-x_L and Bim in stage-specific erythroblasts directly in erythropoietic tissue of fetal and adult mice as they undergo differentiation and respond to stress in vivo. We found a similar, highly dynamic activation of the Bim and Bcl-x_L survival pathways in the fetus that was dependent on both developmental day and erythroblast differentiation stage. These pathways diverge, however, in the adult, where their contrasting dynamic responses suggest a clear segregation of function during the acute and chronic phases of the stress response.

Methods

Mice

Stat5$^{-/-}$ mice were obtained from Dr Lothar Hennighausen (National Institute of Diabetes and Digestive and Kidney Diseases, Bethesda, MD). β-thalassemia mice and the ts-VHL$^{-/-}$ mice were described previously.[5] Bim$^{-/-}$ mice: B6.129S1-Bcl2l11$^{tm1.1Ast}$/J were purchased from The Jackson Laboratory. EpoR-H and EpoR-HM mice were obtained from Dr Jim Ihle (St Jude Children's Research Hospital, Memphis, TN).[35] In all experiments, mice were matched for the same background strain and embryonic age. For low oxygen chamber experiments, Balb/C male littermates of 6 to 11 weeks of age were used. All experiments were conducted in accordance with animal protocol A-1586 approved by the University of Massachusetts Medical School institutional animal care and use committee.

Erythropoietic stress

Recombinant human Epo (Epoetin alfa; Amgen) was injected subcutaneously in a total volume of 150 μL in sterile isotonic saline. Reduced atmospheric oxygen treatment was conducted using the BioSpherix A-chamber (BioSpherix). Hypoxia was achieved by displacing oxygen with nitrogen at normal atmospheric pressure. Temperature, humidity, and carbon dioxide readings were monitored.

Flow cytometry

Flow cytometry was performed on freshly explanted fetal liver, bone marrow (BM), or spleen, as described.[5,18] See supplemental Methods (available on the *Blood* Web site; see the Supplemental Materials link at the top of the online article) for additional detail.

Results

Erythroid developmental delay in Stat5$^{-/-}$ embryos

The definitive erythropoietic lineage generates enucleated red cells and first begins in the murine fetal liver on embryonic day 11.5 (E11.5). Using cell-surface markers CD71 and Ter119, we divided fresh fetal liver into a developmental sequence of increasingly mature subsets S0 to S5[36] (Figure 1A). Most S0 cells (≥ 70%) are erythroid progenitors at the CFU-e stage, just preceding the onset of Epo/EpoR dependence that takes place at the transition from S0 to S1.[36] Subsets S1 to S5 are composed entirely of Epo-dependent erythroid progenitors and precursors. S1 contains CFU-e, S2 contain proerythroblasts, and S3 to S5 contain increasingly mature erythroblasts.[36] Between E11.5 and E14.5, fetal liver cell number increases 1000-fold, principally as a result of increasing numbers of mature erythroblasts[18] (Figure 1A). We previously showed that these rapid changes are associated with apoptosis whose rate varies with both differentiation stage and developmental day.[18]

Given this dynamic picture, we characterized the developmental day and maturation stage–specific expression of Bcl-x_L and Bim in wild-type and Stat5$^{-/-}$ mice (Figure 1). Stat5$^{-/-}$ mice[37] are anemic in utero leading to perinatal death, a similar but more severe phenotype to that of the hypomorphic Stat5 mice.[8,13] CD71/Ter119 profiles on sequential developmental days showed delayed progression from the S1 to S3 (Figure 1A-B, supplemental Figure 1). Specifically, on E12.5, the S1 subset contained only 10% of wild-type fetal liver cells, but 35% of the Stat5$^{-/-}$ fetal liver cells ($P < .005$), while the more mature S3 subset contained ≥ 60% of wild type, but only 20% Stat5$^{-/-}$ fetal liver ($P = .005$). This pattern was not caused by delayed expression of Ter119 or CD71, as evident from cell-size analysis of the S1 and S3 subsets using the flow cytometric forward scatter parameter, which was unaltered for cells in each respective subset (not shown). The slow appearance of S3 cells in the Stat5$^{-/-}$ fetal liver suggests that absence of Stat5 signaling causes a delay in maturation of early (S1) to later (S3/S4-5) erythroid stages in the fetal liver. This effect may be caused by the known functions of Stat5 in iron uptake[38,39] and in antiapoptosis,[8,13,20] and may underlie the previously noted reduced cellularity of the Stat5$^{-/-}$ fetal liver.[39] Of note, S3 cells in E11.5 fetal liver are likely to contain yolk sac cells, which become numerically negligible, compared with definitive lineage cells, in subsequent developmental days.[18,36]

Bcl-x_L and Bim expression in fetal liver is differentiation-stage and embryonic-day dependent

We assessed Bcl-x_L and Bim protein expression using intracellular flow cytometry (Figure 1C-D), using an anti–Bcl-x_L Ab that we previously verified for its specificity[13] (supplemental Figure 2), and an anti-Bim Ab whose specificity we verified using Bim$^{-/-}$ spleen erythroblasts (supplemental Figure 3). Consistent with previous findings in vitro,[20,22] Bcl-x_L expression was low in S0-S2, increasing with differentiation (Figure 1C-D top panels). In addition, Bcl-x_L expression was highly dependent on developmental day, with high levels in S0-S2 on E11.5, decreasing rapidly in the same subsets with embryonic age (Figure 1D top panel).

Bim expression was also dependent on both differentiation stage and embryonic day. Bim expression increased significantly with the transition from S0 to S1, at the onset of Epo and EpoR dependence.[36] The increase was of both the long (Bim_L) and extra-long (Bim_{EL}) transcripts (supplemental Figure 4A, $P < .001$) and in the Bim protein (Figure 1D bottom panel, $P < .0001$). This raised the possibility that Bim induction may be the cause of EpoR dependence. However, we found no significant differences in Epo dependence or in the sensitivity of Bim$^{-/-}$ fetal liver erythroid progenitors to Epo using a CFU-e assay in vitro (supplemental Figure 4B).

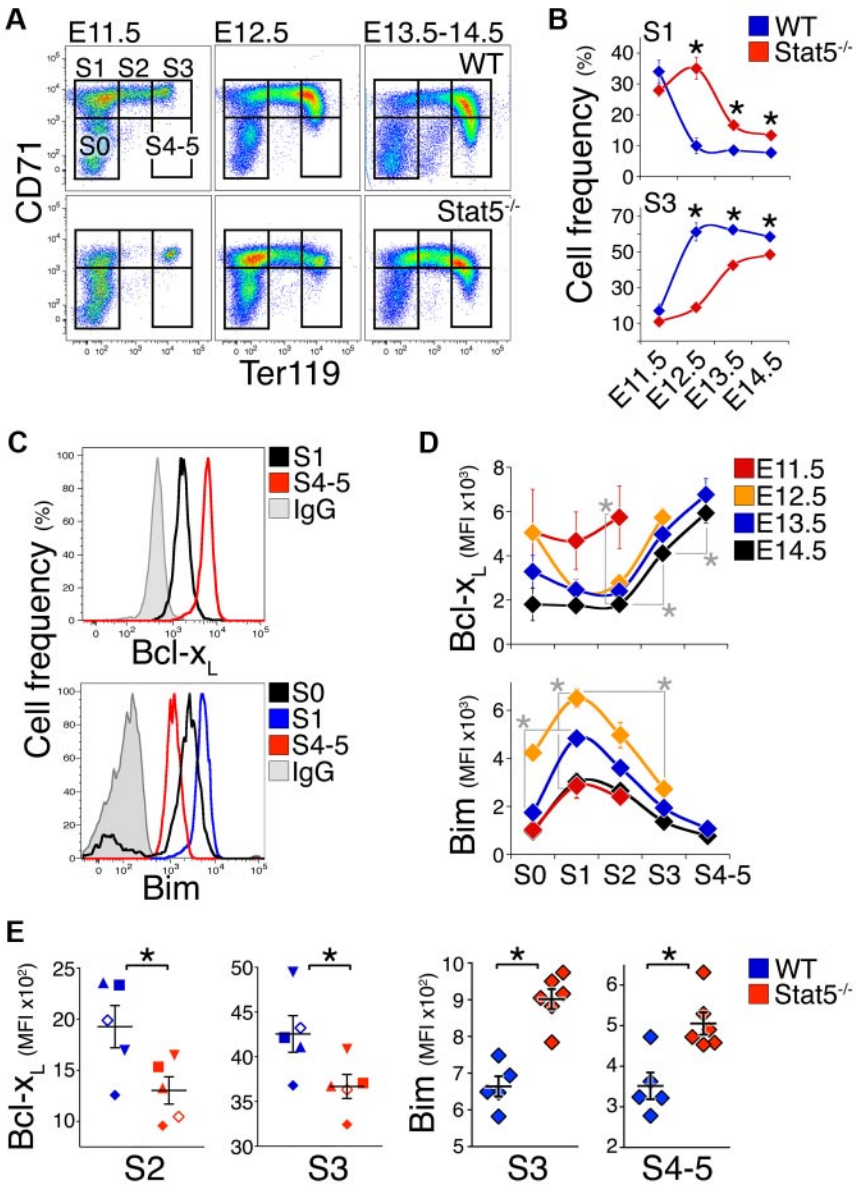

Figure 1. Delayed maturation and altered Bcl-x_L and Bim expression in Stat5$^{-/-}$ fetal liver. (A) Representative flow cytometric CD71/Ter119 fluorescence profiles of Stat5$^{-/-}$ fetal livers and wild-type littermates freshly isolated on consecutive embryonic days (E11.5 to E14.5). S0 to S4/5 are increasingly differentiated erythroid progenitors and precursors subsets in the fetal liver.[36] Dead cells were excluded using LIVE/DEAD viability dye. (B) Summary of analysis performed as in panel A. Data points are each mean ± SEM of 4 to 21 embryos. Statistically significant differences between wild-type and Stat5$^{-/-}$ subsets (⋆) were found for S1 on E12.5 ($P = .002$, 2-tailed t test, unequal variance), E13.5 ($P = .00001$), and E14.5 ($P = .014$) and for S3 on E12.5 ($P = .005$), E13.5 ($P = .00004$), and E14.5 ($P = .010$). (C) Representative flow cytometry histograms for the Bcl-x_L and Bim proteins in the indicated fetal liver subsets. Freshly isolated wild-type E14.5 fetal liver cells were stained with CD71, Ter119, and the LIVE/DEAD viability dye, and were then fixed, permeabilized, and stained intracellularly with an anti–Bcl-x_L antiserum or nonimmune antiserum control (IgG), or with anti-Bim Ab or IgG isotype control. The x-axis is in fluorescence units. (D) Bcl-x_L and Bim protein levels, measured as in panel C, in fresh wild-type fetal liver subsets S0 to S4/5 at the indicated embryonic days. Data were pooled from several experiments with multiple litters. Data points are each the median fluorescence intensity (MFI) ± SEM of 4 to 14 embryos or 6 embryos for Bcl-x_L and Bim measurements, respectively. Nonspecific background fluorescence, defined as the MFI of the corresponding subset stained with control IgG, was subtracted. On E13.5 and E14.5, there were significant differences between S2 and S3 ($P \leq .0001$), and between S3 and S4/5 ($P < .001$, paired t test). Statistically significant differences in Bim expression were found for S1 between E11.5 and E12.5 ($P < .0001$, 2-tailed t test, unequal variance). On E12.5, there were significant differences between S0 and S1 ($P < .0001$), and between S1 and S3 ($P < .0001$). Similar developmental patterns were observed in C57BL/6 and Balb/C backgrounds. (E) Lower Bcl-x_L and higher Bim levels in E14.5 Stat5$^{-/-}$ embryos compared with wild-type littermate controls, at the indicated differentiation subset. For Bcl-x_L, n = 11 to 21 embryos per genotype, with each symbol type representing median expression for 1 litter. Means ± SEM for the population are indicated. Statistically significant differences were found for S2 ($P = .03$), S3 ($P = .002$, paired t test). For Bim, data points are individual embryos. Mean ± SEM for the population is shown. Statistically significant differences were found for S3 and S4-5 ($P < .01$, 2-tailed t test, unequal variance).

Bim protein expression peaks in S1 and is gradually suppressed with erythroid differentiation, reaching its lowest values in mature erythroblasts (Figure 1D bottom panel). In addition, for a given maturation subset, Bim is lowest on E11.5, peaking on E12.5, and decreasing in older embryos (Figure 1D). The developmental age–dependent changes in Bcl-x_L and Bim are consistent with similar changes in apoptosis, cell number, and Fas expression.[18]

Bim and Bcl-x_L expression in fetal liver is regulated by Stat5

The rapidly changing expression of Bim and Bcl-x_L during E11.5-E12.5 (Figure 1D), and the developmental delay in the Stat5$^{-/-}$ fetal liver (Figure 1A-B, supplemental Figure 1), together impede our ability to assess the role of Stat5 in regulating Bim and Bcl-x_L expression. However, by E13.5, Bim and Bcl-x_L expression stabilizes, and the Stat5$^{-/-}$ CD71/Ter119 fetal liver profile approaches that of wild-type embryos (Figure 1D, A, and B, respectively). We therefore compared Bim and Bcl-x_L expression in Stat5$^{-/-}$ fetal liver and wild-type littermates on E13.5-E14.5 (Figure 1E, supplemental Figure 4C-D).

Bcl-x_L expression in the Stat5$^{-/-}$ fetal liver was 1.5- to 2-fold lower in the early erythroblast subsets S1 ($P = .01$), S2 ($P = .03$), and S3 ($P = .002$). Bim levels in Stat5$^{-/-}$ fetal liver were 30% and 40% higher, respectively, in the S3 and S4/5 subsets ($P < .01$), suggesting Stat5 regulates its expression. For comparison, we also assessed expression of the erythroblast apoptotic regulators Fas and FasL in the Stat5$^{-/-}$ fetal liver. We found no significant difference in Fas expression between Stat5$^{-/-}$ embryos and wild-type littermates (supplemental Figure 5).

Bcl-x_L is rapidly induced in adult early erythroblasts in response to a single Epo injection

To investigate adult erythropoietic tissue, we used cell-surface markers CD71 and Ter119, as in the fetal liver, together with the forward scatter parameter. The contours of the adult flow cytometric CD71/Ter119 histogram differ from those of the fetal liver (Figures 2B and 1A, respectively). We subdivide adult erythroid cells into subsets ProE, EryA, EryB, and EryC[5,17] (Figure 2B). These correspond, approximately, to proerythroblasts, early and

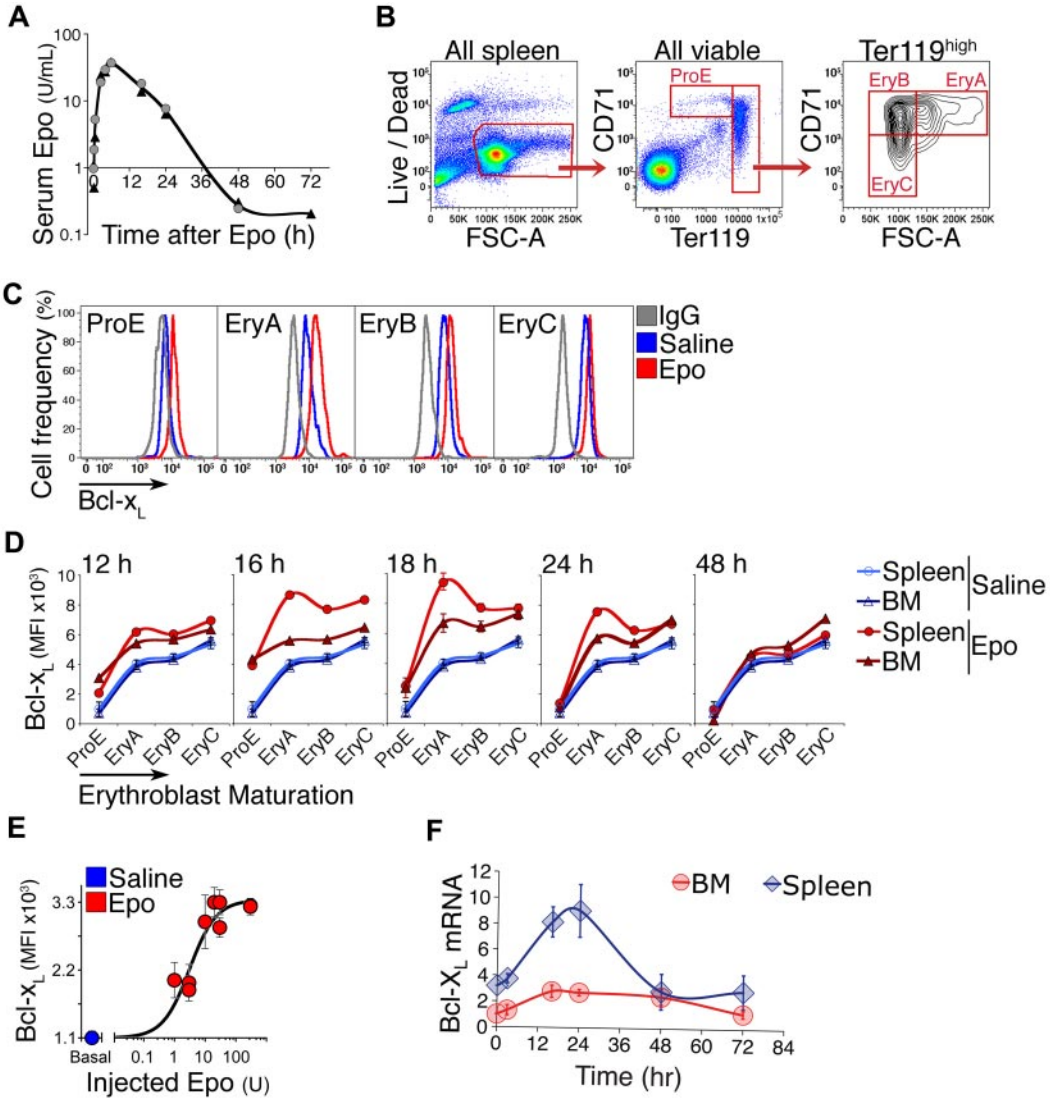

Figure 2. Bcl-x_L is induced in adult early erythroblasts in response to Epo injection. (A) Time course of plasma Epo, assayed by ELISA, after a single subcutaneous injection of 300 U/25 g body weight. Two mice (identified as either circles or triangles) were assayed per time point. (B) Gating strategy for freshly explanted adult splenic erythroid subsets ProE, EryA, EryB, and EryC.[5] Live cells were selected, and subsets gated based on Ter119, CD71, and forward scatter (FSC). The spleen illustrated in this panel was harvested 18 hours after a subcutaneous Epo injection. All axes units refer to fluorescence. (C) Representative flow cytometric histograms of Bcl-x_L in the indicated spleen erythroblast subsets. Anti–Bcl-x_L antiserum was used to stain erythroblasts from a saline-injected mouse (blue histograms), or an Epo-injected mouse (300 U/25 g, red histograms) in freshly explanted spleen at 18 hours postinjection. Nonimmune serum (IgG) was used to measure the nonspecific binding in each subset (gray histograms). The x-axis is in fluorescence units. (D) Bcl-x_L expression measured as in panel C in freshly explanted spleen, in each erythroblast subset at each of the indicated time points after a single Epo injection (300 U/25 g). Each data point for Epo-injected mice is mean ± SEM of n = 4 mice for t = 16, 18, 24, 48 hours, and mean of 2 mice for t = 12 hours. Blue curves are mean ± SEM of n = 14 saline-injected mice pooled from all time points. The same blue curves are reproduced for comparison with Epo-injected mice at each time point. Statistical significance values: ProE at t = 16 hours, in BM *P = .005, in spleen *P = .0006. EryA in spleen, *P = .0009 at 16 hours, *P = .0009 at 18 hours. EryA in BM, *P = .013 at 16 hours, *P = .015 at 18 hours. The induction of Bcl-x_L in splenic EryA was significantly higher than in BM EryA (*P = .021). Two-tailed t test with unequal variance was used for all comparisons. (E) Epo dose/Bcl-x_L response in vivo in spleen EryA. Wild-type Balb/C mice were injected subcutaneously with either saline (= basal, blue circle) or a single dose of Epo (1, 3, 10, 20, 30, or 300 U/25 g, red circles). Bcl-x_L was measured by flow cytometry as in panel C at 18 hours postinjection, with the nonspecific fluorescence reading subtracted for each subset. Data from 2 independent experiments were pooled and normalized. Data points were fitted with a Hill curve. Each data point represents mean ± SEM of n = 3 to 4 mice. (F) Time course of Bcl-x_L mRNA levels after a single Epo injection (300 U/25 g), in freshly isolated and sorted spleen and BM EryA. Quantitative real-time PCR (qRT-PCR), data points are mean ± SEM of 3 independent experiments. Data are expressed relative to the β-actin mRNA and normalized to the value in BM EryA in saline-injected mice.

late basophilic erythroblasts, and polychromatic/orthochromatic erythroblasts, respectively.[5] With this methodology, we examined Bcl-x_L expression in response to Epo. A single subcutaneous Epo injection (300 U/25 g) results in a rapid increase in serum Epo, which peaks by 6 hours, persists for 24 hours, and declines to baseline by 36 hours (Figure 2A). We assessed changes in Bcl-x_L in freshly explanted BM and spleen erythroblasts at the indicated time points (Figure 2C-D). In control uninjected or saline-injected mice, Bcl-x_L levels are lowest in ProE, increasing gradually with maturation and reaching 6-fold higher levels in the most mature, EryC subset (Figure 2D blue curves; supplemental Figure 6; representative histograms in Figure 2C, summary of several experiments in Figure 2D). Injected Epo altered this pattern, causing a further induction of Bcl-x_L expression in all erythroblast subsets (Figure 2C-D). The largest and most rapid increase was in the earliest subsets, where basal Bcl-x_L levels are lowest. Thus, Bcl-x_L induction peaked 5-fold within 16 hours of Epo injection in splenic ProE (P = .0006) and 3-fold by 18 hours in splenic EryA, where it reached its highest expression levels (P = .0009; Figure 2C-D).

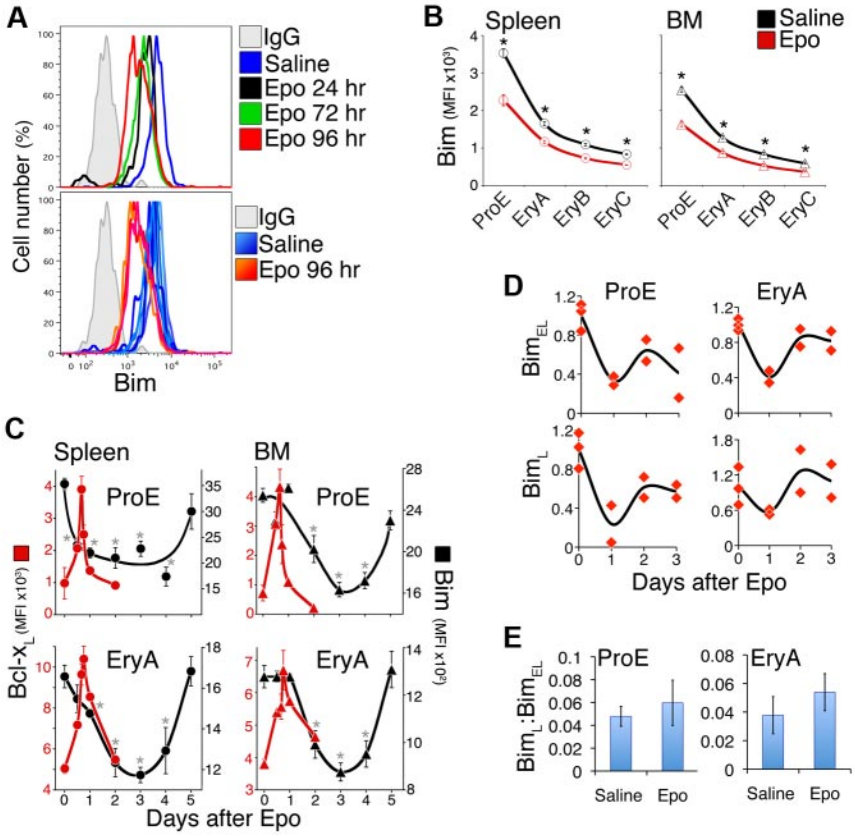

Figure 3. Transient Bcl-x_L induction contrasts with slower Bim suppression in response to Epo injection. (A) Flow cytometric histograms of Bim in freshly harvested splenic ProE. (Top panel) Histograms corresponding to single mice at the indicated time points after Epo injection, or 24 hours after control saline injection. Bim levels decrease (histograms shift to the left) after Epo injection. (Bottom panel) Bim levels in 6 saline-injected mice (6 histograms in various shades of blue) and 3 Epo-injected mice (histograms in shades of red/orange). The x-axis is in fluorescence units. (B) Bim protein levels, measured as illustrated in panel A, in adult erythroid differentiation subsets 3 days after a single injection of either Epo (red, 300 U/25 g) or saline (black). Data are mean ± SEM of n = 21 mice for saline injection, and n = 10 mice for Epo injection. *$P < .00001$ (2-tailed *t* test, unequal variance) for differences between Epo and saline-injected mice. (C) Time course of Bcl-x_L up-regulation (red symbols, plotted on the left, red-numbered y-axis) and Bim suppression (black symbols, plotted on the right, black-numbered y-axis) in spleen (circles) and BM (triangles) in response to a single Epo injection (300 U/25 g) on day 0. Includes a subset of the data plotted in panel B (for Bim) and Figure 2D (for Bcl-x_L). Bim data are mean ± SEM of n = 21 mice for day 0, and n = 3 to 10 mice for days 1 to 5, pooled from 5 experiments. Bim ProE curves (black lines) for spleen and BM were hand-drawn. Bim on day 0 was significantly different from subsequent days, where indicated: spleen ProE: *$P < .005$; spleen EryA: *$P < .025$; BM ProE: *$P < .02$; BM EryA: *$P < .01$ (2-tailed *t* test, unequal variance). (D) Time course of Bim_L and Bim_{EL} mRNA levels after a single Epo injection (300 U/25 g), in freshly isolated and sorted BM EryA and ProE. Each data point is the mean of triplicate qRT-PCR measurements on sorted cells from individual mice, expressed relative to the β-actin mRNA and normalized to t = 0 (saline-injected mice). There was a significant decrease after Epo injection in Bim_{EL} mRNA in ProE ($P = .00439$, 2-tailed *t* test, unequal variance, all post-Epo injection data were pooled) and EryA ($P = .013$), and in Bim_L mRNA in ProE ($P = .027$). (E) The ratio of Bim_L to Bim_{EL} mRNA in Epo-injected and in saline-injected mice, in the experiments described in panel D. Data are mean ± SD; all Epo time points were pooled for the purpose of this analysis. There were no significant changes in this ratio with Epo injection.

We carried out a dose/response curve in vivo, examining peak Bcl-x_L in splenic EryA at 18 hours following injection of various Epo doses (Figure 2E). Half the maximal response was obtained when injecting 3 U/25 g, estimated to result in a serum concentration of 0.3 U/mL, an ~ 10-fold increase in serum Epo.

Up-regulation of the Bcl-x_L protein in spleen EryA was associated with increased Bcl-x_L mRNA with a similar time course. There was a lower absolute level of the Bcl-x_L mRNA in BM (Figure 2F).

Bim expression in adult basal and stress erythropoiesis

We examined Bim expression in adult spleen and BM, freshly explanted at the indicated time points after either saline or Epo injection (300 U/25 g). Bim expression is highest in the ProE subset, declines with differentiation, and reaches a quarter of its ProE level in EryC (Figure 3A-B). In response to Epo, Bim levels decreased further in all subsets (Figure 3A-C), with the largest decline in BM and spleen ProE progenitors, where they fell 1.5- to 2-fold ($P < .00001$).

Importantly, in most subsets the time course of Bim suppression in response to Epo injection was much slower, and more prolonged, than the Bcl-x_L response. Maximal Bim suppression was reached at 72 hours after injection, by which time Bcl-x_L induction had peaked and returned to baseline (Figure 3C).

We also examined Bim mRNA in sorted BM ProE and EryA of mice injected with Epo. Like the Bim protein, both Bim_L and Bim_{EL} decreased by ~ 2-fold. There was little change in the Bim_L:Bim_{EL} ratio (Figure 3D-E).

The erythroblast response to reduced atmospheric oxygen

The modulation of erythroblast Bim and Bcl-x_L by Epo in vivo suggested that they may play a role in the physiologic stress response. To test this, we placed mice in a reduced oxygen environment in which partial oxygen pressure was reduced to 11% for up to 5 days (Figure 4). Epo levels in blood plasma rose in the first 24 hours from a basal level of 12 mU/mL, to a peak of 29 mU/mL ($P = .001$). This high Epo level was sustained until day

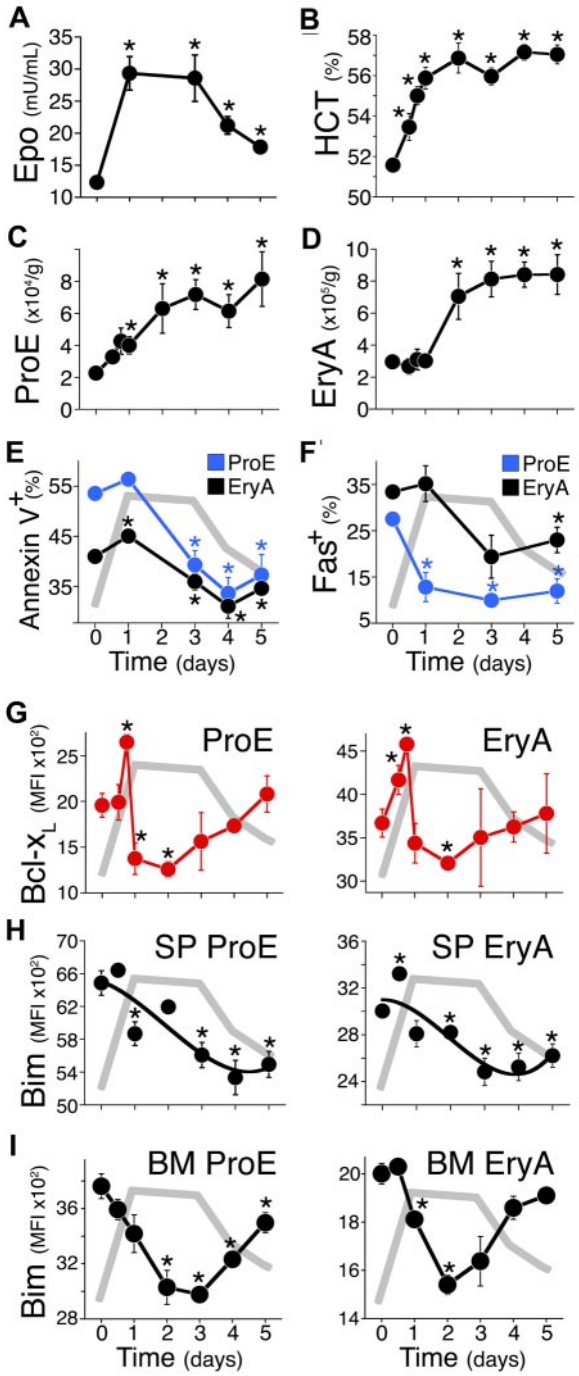

Figure 4. A reduced-oxygen environment elicits a rapid, transient Bcl-x_L induction and a slower, persistent Bim suppression. (A-I) Mice were placed in a low oxygen chamber (11%) on day 0, for up to 5 days. (A) Endogenous plasma Epo, assayed by ELISA. Data are mean ± SEM. Epo was significantly elevated relative to day 0 (n = 27 mice) on all subsequent days (n = 6 to 12 mice per time point, $P < .006$, 2-tailed *t* test, unequal variance). The Epo time course is redrawn in gray in panels E to I. (B) Daily hematocrit (HCT) of blood collected immediately after euthanasia. Data are mean ± SEM of n ≥ 6 mice per time point. Differences from day 0 were significant at 12 hours ($P = .019$), 18 hours to day 5 ($P < .0002$). (C-D) Spleen ProE and EryA (cell number per gram body weight). Data pooled from 23 independent experiments. Each data point is mean ± SEM of n ≥ 6 mice. Differences from day 0 (n = 82 mice) were significant for ProE on day 1 ($P = .005$), day 2 ($P = .047$), days 3 to 5 ($P \leq .005$), and for EryA on day 2 ($P = .034$), days 3 to 5 ($P \leq .001$). (E) Annexin V binding in spleen ProE (blue) and EryA (black). Data points are mean ± SEM of 33 mice for day 0, and 3 to 7 mice for subsequent days, pooled from 2 to 5 independent experiments per day. Differences from day 0 are significant for ProE on days 3 to 5 ($P \leq .002$), and for EryA on day 1 ($P = .001$) and days 3 to 5 ($P = .03$, 0.02, 0.001, respectively). (F) Fas-positive cell frequency in spleen ProE (blue) and EryA (black), measured by flow cytometry in freshly explanted tissue. 3. On days 4 and 5, Epo began to decline to a new lower plateau of 18 mU/mL (Figure 4A).

The hematocrit response was rapid, rising from 51.5% to 56% in the first 24 hours, and reaching a sustained plateau of 57% (Figure 4B). This rapid initial increase is likely to be in part caused by plasma volume adjustment in response to hypoxia.[40,41]

We examined the response to hypoxia of specific erythroblast subsets in freshly explanted tissue (Figure 4C-I). The results shown are from 23 pooled experiments, with at least 6 mice per time point. During the first 3 days, there was an increase in the absolute numbers of spleen ProE and EryA erythroblasts, reaching new plateaus that were 4- and 3-fold higher than basal values, respectively (Figure 4C-D). This increase was associated with a marked and significant decrease in apoptosis, with the number of Annexin V^+ cells declining from 55% to 32% ($P = .002$) and 42% to 30% ($P = .001$) in the ProE and EryA, respectively (Figure 4E).

The response of erythroblast Bim, Fas, and Bcl-x_L to reduced atmospheric oxygen

Given the clear changes in ProE and EryA apoptosis, we investigated their expression of the apoptotic regulators Fas, Bim, and Bcl-x_L. We previously showed that Fas expressed by spleen ProE and EryA decreases in response to several acute and chronic erythropoietic stress conditions. Maximal Fas suppression is reached within 24 to 48 hours and is maintained for the duration of the stress stimulus (Figure 4F).[5,19]

The Bcl-x_L response was rapid and transient, its expression peaking by 18 hours in both ProE and EryA, and then rapidly dipping below baseline by 24 hours, in spite of the persisting high Epo levels (Figure 4G). The response of Bim, by contrast, was slower, reaching maximal suppression at 48 hours, with low levels maintained for the duration of high Epo levels (Figure 4H-I).

Response of the Bim and Bcl-x_L pathways to chronic erythropoietic stress

We went on to assess the Bim and Bcl-x_L response to chronic erythropoietic stress. The Bcl-x_L expression in the ProE/EryA-C subsets in either spleen or BM was unaltered by 3 distinct erythropoietic stress conditions: pregnancy at mid-gestation, chronic anemia caused by β-thalassemia,[42] and chronic erythrocytosis caused by tissue-specific deletion of the von Hippel-Lindau gene that results in elevated Epo (ts-$VHL^{-/-}$)[43] (Figure 5A). Plasma Epo is elevated to 30 mU/mL and 220 mU/mL in the ts-$VHL^{-/-}$ and β-thalassemia mice, respectively (supplemental Figure 7), a concentration range sufficient for up-regulation of Bcl-x_L in acute stress (Figure 4). Furthermore, we have previously shown that cell-surface Fas and FasL are down-regulated in the same chronic stress models.[5]

Figure 4 (continued) Data are mean ± SEM of n = 26 mice pooled from 4 experiments (day 0), or n = 3 mice for subsequent days. Differences from day 0 were significant for ProE on day 1 ($P = .024$), day 3 ($P < .00001$), day 5 ($P = .001$), and for EryA on day 5 ($P = .04$). (G) Bcl-x_L protein in spleen ProE and EryA measured by flow cytometry in freshly explanted tissue. Data pooled from 3 independent experiments. Each data point is mean ± SEM of n ≥ 3 mice. Differences from day 0 (n = 17) are significant for ProE at 18 hours (n = 3, $P < .001$), 24 hours (n = 7, $P = .019$), 48 hours (n = 5, $P < .0005$), and for EryA, at 12 hours ($P = .046$), 18 hours ($P < .0001$), 48 hours ($P = .02$). (H-I) Bim protein expression in spleen (H) and BM (I) ProE and EryA, measured by flow cytometry in freshly explanted tissue. Data are mean ± SEM of n ≥ 3 mice. Differences from day 0 were significant for spleen ProE on day 1 ($P = .014$), days 3 to 5 ($P \leq .005$), spleen EryA on day 0.5 ($P = .0014$), days 2 to 5 ($P < .04$), BM ProE on day 2 ($P = .007$), day 3 ($P < .00001$), day 4 ($P < .001$), day 5 ($P = .04$), BM EryA on day 1 ($P = .002$), day 2 ($P = .0001$), day 3 ($P = .05$).

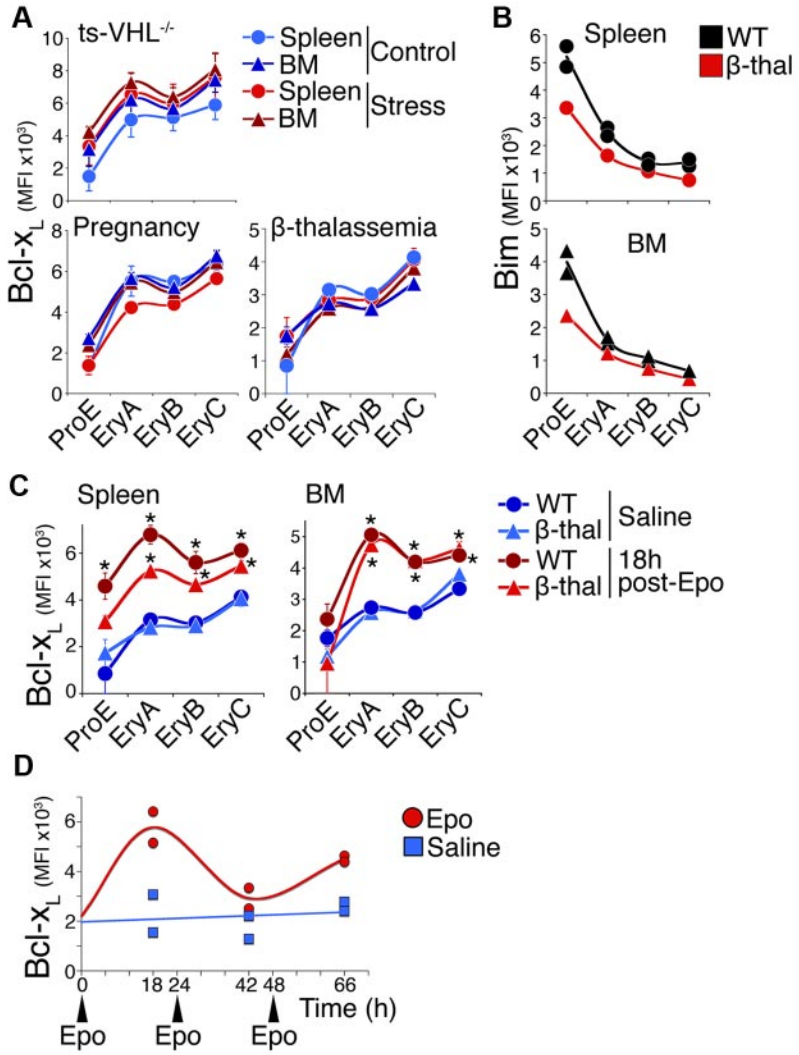

Figure 5. The Bcl-x_L response to chronic stress and to acute-on-chronic stress. (A) Bcl-x_L expression in mouse models of erythropoietic stress (red symbols) and matched controls (blue symbols), measured in freshly explanted tissue. Each data point is mean ± SEM of 2 to 4 mice. There were no statistically significant differences between chronic stress and control mice. (B) Representative experiment showing Bim expression in β-thalassemia mice in spleen (top) and BM (bottom). Two wild-type (black symbols) and 1 β-thalassemia mouse (red symbols) are shown. (C) The Bcl-x_L response to an acute-on-chronic stimulus. Bcl-x_L was measured in spleen and BM erythroblasts in β-thalassemia and matched control mice, 18 hours after a single injection of either Epo (300 U/25 g, red symbols) or saline (blue symbols). Data points are mean ± SEM of n = 3 to 4 mice. Representative of 4 independent experiments. There were statistically significant differences in Bcl-x_L between Epo and saline injections in wild-type spleen ProE ($P = .025$, 2-tailed t test, unequal variance), EryA ($P = .0009$), EryB ($P = .01$), and EryC ($P = .006$); in β-thalassemia spleen EryA ($P = .0004$), EryB ($P = .004$), and EryC ($P = .03$); in wild-type BM EryA, EryB, and EryC ($P \leq .0005$); and in β-thalassemia BM EryA, EryB ($P < .0005$), and EryC ($P = .025$). The increase in spleen EryA Bcl-x_L was significantly higher ($P = .023$) in wild-type mice than in β-thalassemia mice. (D) The Bcl-x_L response to 3 consecutive Epo injections. Wild-type mice were injected at time points 0, 24, and 48 hours with either Epo (300 U/25 g, indicated with arrowheads) or with saline. Bcl-x_L in spleen EryA was assayed by flow cytometry in 2 mice for each treatment, 18 hours after each injection.

Unlike Bcl-x_L, Bim expression in the β-thalassemia mice was suppressed in all erythroblast subsets (Figure 5B), to levels similar to those seen in response to an acute Epo injection (Figure 3B).

The Bcl-x_L response to an "acute-on-chronic" stress stimulus

The transience of the Bcl-x_L response to stress is reminiscent of sensory systems that undergo adaptation, such as neutrophil chemotaxis or sensory neural adapting systems. These systems respond to a change in the stimulus, rather than to absolute stimulus levels.[44] We therefore asked whether the desensitization of the Bcl-x_L pathway to chronic stress was permanent, or whether an acute change in the level of stress, superimposed on a chronic stress stimulus, would restimulate Bcl-x_L induction.

We injected β-thalassemia mice with Epo at 300 U/25 g, and examined Bcl-x_L expression at 18 hours. We found clear induction of Bcl-x_L in all erythroblast subsets in the β-thalassemia mice, closely resembling that of control mice in the BM, and only a little short of the wild-type response in the spleen (Figure 5C). Therefore, while the Bcl-x_L response to chronic stress is desensitized, it responds rapidly to new changes in stress superimposed on the chronic stress levels.

To further define the Bcl-x_L response to stress, we examined mice injected with Epo (300 U/25 g) daily for 3 consecutive days, and measured the Bcl-x_L response at 18 hours following each injection (Figure 5D). The Bcl-x_L response to the second and third Epo injections was either absent or diminished compared with the first injection (Figure 5D). Therefore, a new increase in Epo that occurs close to a previous episode of stress does not elicit Bcl-x_L up-regulation. This experiment suggests that the Bcl-x_L response to acute stress is followed by a refractory period of at least 24 hours during which Bcl-x_L fails to respond further to new changes in Epo or stress.

Stat5 activation in vivo undergoes adaptation

We asked whether adaptation in the Bcl-x_L stress response is caused by adaptation in Stat5, its upstream regulator. We examined the time course of Stat5 activation in vivo after Epo injection (300 U/25 g), using intracellular flow cytometry in freshly explanted spleen (Figure 6A). We validated the specificity of the anti-phospho-Stat5 Ab to the phosphorylated Y694 C-terminal residue of Stat5 (supplemental Figure 8). The number of ProE and EryA containing active, phosphorylated Stat5 (p-Stat5) increased rapidly after Epo injection, peaking by 30 minutes, but declining rapidly to a lower level by 6 hours (Figure 6A). Of note, plasma Epo peaked at 6 hours (Figure 2A), suggesting the decline in p-Stat5 is intrinsic to the p-Stat5 response and not caused by declining Epo.

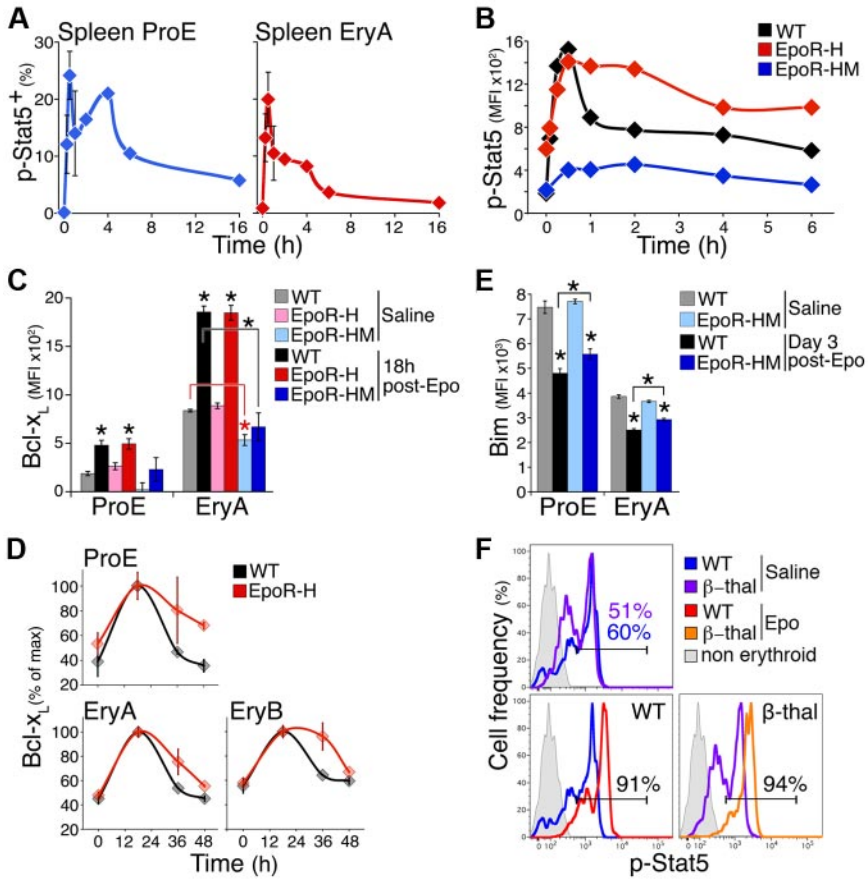

Figure 6. Adaptation in the Bcl-x_L and p-Stat5 responses is dependent on the EpoR C-terminal cytoplasmic domain. (A) The p-Stat5 response to Epo in vivo in freshly explanted spleen ProE and EryA at the indicated times after a single Epo injection (300 U/25 g). Data were pooled from 4 independent experiments. Each time point is the mean ± SEM of data from 2 to 4 mice. (B) The p-Stat5 time course in S1 fetal liver cells in response to Epo stimulation (2 U/mL), shown for EpoR-HM, EpoR-H, and matched wild-type fetal livers at E13.5. Data are MFI above background (isotype-control Ab). Representative of 3 similar experiments. (C) The Bcl-x_L response to Epo in vivo in EpoR-H and EpoR-HM mice. Bcl-x_L was measured 18 hours after a single injection of either saline or Epo (300 U/25 g), in freshly explanted spleen ProE and EryA of EpoR-H, EpoR-HM, or wild-type controls. Data are mean ± SEM of n = 3 to 5 mice per bar. Significant Bcl-x_L increase from basal levels in spleen ProE and EryA was seen in Epo vs saline-injected wild-type (black) and EpoR-H (red) mice (stars without brackets: WT ProE *$P = .003$; EpoR-H ProE *$P = .012$; WT EryA *$P = .00004$; EpoR-H EryA *$P = .0001$, 2-tailed t test, unequal variance), but not in EpoR-HM mice (blue). Bcl-x_L was reduced in basal state EpoR-HM spleen EryA (red star with red bracket, *$P = .027$) compared with wild-type basal control. Bcl-x_L induction in wild-type spleen EryA was significantly above that of EpoR-HM EryA (black star with bracket, *$P = .007$). (D) Time course of the Bcl-x_L response in EpoR-H mice and in matched wild-type controls, after a single Epo injection (300 U/25 g). Measurements were made in freshly explanted spleen at the indicated time points. Bcl-x_L is significantly higher in EpoR-H at 36 and 48 hours ($P < .005$, paired t test on all subsets). (E) Bim protein in spleen ProE and EryA of wild-type and EpoR-HM mice on day 3 after a single Epo injection (300 U/25 g). Data are mean ± SEM of n = 4 to 5 mice per bar. There was no significant difference in basal Bim between EpoR-HM and wild-type control mice. Bim was significantly suppressed after Epo injection (*$P < .001$). Bim was suppressed by a significantly smaller extent in EpoR-HM ProE and EryA subsets (stars with brackets, *$P = .03$ and *$P = .001$, respectively, 2-tailed t test, unequal variance). (F) The p-Stat5 histograms in vivo at peak response (30 minutes) after a single injection of either Epo (300 U/25 g) or saline, in either β-thalassemia mice or in matched wild-type controls, measured in freshly explanted spleen ProE. The p-Stat5$^+$ gate was drawn based on the nonerythroid population in spleen (gray histograms). The x-axis is in fluorescence units.

Signal adaptation may be the result of negative feedback.[45,46] p-Stat5–mediated transcriptional activation of SOCS family proteins results in feedback inhibition of the Jak2 and Stat5 response.[47] This negative regulation in part depends on SOCS protein binding to phosphotyrosines on the activated EpoR cytoplasmic domain.[2] To investigate the possibility that Stat5-mediated negative feedback is responsible for p-Stat5 adaptation, we investigated two knock-in mouse models expressing the EpoR mutants EpoR-H and EpoR-HM,[35] both lacking the negative regulatory distal portion of the EpoR cytoplasmic domain containing 7 of its 8 phosphotyrosines, including SOCS family docking sites.[2] In EpoR-HM, the remaining Y343, a Stat5 docking site, is mutated to phenylalanine.[35] The EpoR-H mouse has a mildly elevated basal hematocrit. The EpoR-HM mouse has a mild basal anemia and a deficient stress response.[35]

We tested the response of freshly harvested fetal liver erythroblasts from EpoR-H, EpoR-HM, and wild-type embryos to continuous stimulation with Epo for up to 6 hours in vitro. The time course of response of wild-type erythroblasts was similar to that of adult erythroblasts in vivo (Figure 6A-B). The peak p-Stat5 response to Epo stimulation in EpoR-HM erythroblasts was 15% of the response in wild-type or EpoR-H mice, in agreement with previous results.[48] In EpoR-H erythroblasts, peak p-Stat5 was similar to that of the wild-type response, though baseline p-Stat5 was higher. In both EpoR-HM and EpoR-H, duration of the initial p-Stat5 peak was prolonged substantially (Figure 6B). These findings suggested that the distal EpoR cytoplasmic domain, likely through binding to Stat5-induced SOCS family proteins, is responsible for curtailing the p-Stat5 response.

The Bcl-x_L and Bim stress responses in EpoR-H and EpoR-HM mice

The finding that the p-Stat5 signal undergoes adaptation (Figure 6A-B) suggests it may be responsible for the adaptation in the Bcl-x_L response. To test this, we asked whether failure of p-Stat5

adaptation in the EpoR-H mouse (Figure 6B) would prevent adaptation of the Bcl-x_L response.

We injected EpoR-H mice with Epo (300 U/25 g) and examined the resulting induction of Bcl-x_L. The peak Bcl-x_L response was closely similar to that of matched wild-type control mice (Figure 6C, supplemental Figure 9A). There was little increase in Bcl-x_L in EpoR-HM mice, consistent with p-Stat5 as the principal regulator of the Bcl-x_L stress response (Figure 6C, supplemental Figure 9A). Importantly, there was a failure of adaptation of the Bcl-x_L response in EpoR-H mice. Bcl-x_L levels remained elevated well above their initial baseline at 36 and 48 hours postinjection in spleen ProE, and at 36 hours in EryA and EryB ($P < .005$, Figure 6D), even though Bcl-x_L levels in wild-type mice (Figure 6D) and serum Epo (Figure 2A) had returned to baseline. This strongly suggests that adaptation in the Bcl-x_L response requires the EpoR distal cytoplasmic domain and is most likely a result of adaptation in the p-Stat5 response, also dependent on this domain (Figure 6B).

Bim expression was suppressed in EpoR-HM mice in response to a single Epo injection (300 U/25 g). However, suppression was less efficient than in wild-type mice, by a small but statistically significant amount (Figure 6E, supplemental Figure 9B, $P = .03$ and $P = .001$ in ProE and EryA, respectively). These results suggest that, in addition to Stat5, other pathways, likely ERK, regulate EpoR-mediated Bim suppression.[33]

The p-Stat5 response to an acute-on-chronic stress stimulus

Although Bcl-x_L expression is not elevated in chronic stress, it is induced in response to an acute stimulus superimposed on the chronic stress stimulus (Figure 5C). We similarly examined the p-Stat5 response to chronic and acute-on-chronic stress stimuli. We found no increase in the level of p-Stat5 in ProE freshly isolated from β-thalassemic mice (Figure 6F top panel), in spite of the chronically elevated plasma Epo in these mice (supplemental Figure 7). A single injection of β-thalassemic mice with Epo (300 U/25 g), however, resulted in a rapid increase in p-Stat5 in both β-thalassemic mice and in matched control mice (Figure 6F bottom panels). These data further support our conclusion that adaptation in the p-Stat5 response is the cause of adaptation in the Bcl-x_L response to stress.

Discussion

We examined Bim suppression and Bcl-x_L induction, two EpoR-activated erythroblast survival pathways in fetal and adult basal and stress erythropoiesis. Their analysis in vivo revealed previously unsuspected functional specialization of EpoR-activated pathways to either the chronic or acute phases of the stress response. Bcl-x_L induction behaves like a classic sensory adapting pathway, being insensitive to the prevailing level of stress, and instead responding only to changes in stress level. Adaptation allows Bcl-x_L to provide a stop-gap at the onset of stress that rapidly rescues early erythroblasts from apoptosis, until slower but persistent stress pathways, such as Bim or Fas suppression, are activated. Mechanistically, we suggest that adaptation in the Bcl-x_L response is the result of adaptation in the response of p-Stat5, its upstream regulator.

Regulation of Bim and Bcl-x_L expression in early-versus-late erythroblasts

We delineated the expression pattern of both Bim and Bcl-x_L proteins throughout erythroid maturation in adult and fetal tissue in vivo. The basal pattern observed in the absence of stress is one of low Bcl-x_L and high Bim in early erythroblasts, inverting with differentiation so that in mature erythroblasts Bim levels are low and Bcl-x_L levels are high (Figure 7A). These results are consistent with previous reports of increasing Bcl-x_L with differentiation in vitro,[20,22] and with the increase in Bcl-x_L and decrease in Bid and Bax transcripts with the transition from early-to-late erythroblasts in murine BM.[6] Together with our previous findings of high Fas and FasL in early, but not late, erythroblasts,[5,18,49] a strong pattern emerges of apoptosis-prone early erythroblasts, containing high levels of proapoptotic regulators and only low levels of antiapoptotic proteins, gradually transitioning into apoptosis-resistant late erythroblasts in which antiapoptotic proteins predominate. This underlying pattern explains why high levels of apoptosis are seen in early erythroblasts but not in late erythroblasts during normal fetal and basal adult erythropoiesis in vivo[5,18,19,49] (Figure 4E), and was recently suggested as responsible for the sensitivity of early erythroblasts to irradiation.[6]

Bcl-x_L is regulated by both GATA-1 and EpoR-activated Stat5.[23] Similarly, Bim suppression is regulated by EpoR-activated ERK[33] and by GATA-1–induced LRF.[34] In addition, we found that Bim is regulated by EpoR-activated Stat5 in fetal liver and, to a lesser extent, in the adult (Figures 1E, 6E, and supplemental Figure 9B). Lower Bcl-x_L in the S1-S3 subsets of the Stat5$^{-/-}$ fetal liver, and in EpoR-HM mice in the basal state, support the role of Stat5 in the induction of erythroid Bcl-x_L.[8,13,20] The role of Stat5 is especially notable, however, in the Bcl-x_L stress response, which is absent in the EpoR-HM mice (Figure 6C).

Based on these expression patterns, we propose that EpoR and GATA-1–mediated regulation of Bim and Bcl-x_L are largely segregated to the early and late erythroblast compartments, respectively (Figure 7A). Specifically, the underlying, largely stress-insensitive gradual increase in Bcl-x_L and gradual suppression of Bim with differentiation is likely to be mediated by GATA-1. Superimposed on this pattern are Epo-mediated, stress-dependent adjustments that modulate Bcl-x_L induction and Bim suppression in early erythroblasts (Figures 2, 3, and 7A). Thus, only the apoptosis-prone CFU-e, proerythroblasts, and early basophilic erythroblasts (= early erythroblast compartment) are dependent on EpoR signaling for survival in the basal state. Furthermore, during hypoxic stress, it is principally the early erythroblast compartment that is Epo responsive and undergoes expansion as a result of reduced apoptosis[5,18,19,49] (Figure 4E). The susceptibility of the early erythroblast compartment to apoptosis is precisely the characteristic that gives plasticity to the erythropoietic system, allowing the level of EpoR signaling to determine erythropoietic rate. Peak Bcl-x_L protein and mRNA levels in response to stress were attained in EryA erythroblasts in spleen, a subset that is Epo responsive, and that expands dramatically in response to erythropoietic stress.[5] The more prominent response of spleen EryA compared with BM EryA is consistent with the known role of the spleen as the primary site of stress erythropoiesis.

Using Fas and FasL-mutant mice, we found recently that the Epo-mediated Fas suppression accounts for ~ 30% of the early erythroblast expansion in stress.[19] Bim suppression and Bcl-x_L induction are therefore likely to cooperate with Fas suppression, and potentially with other, as yet uncharacterized antiapoptotic pathways, in achieving the full expansion of the early erythroblast compartment during stress.

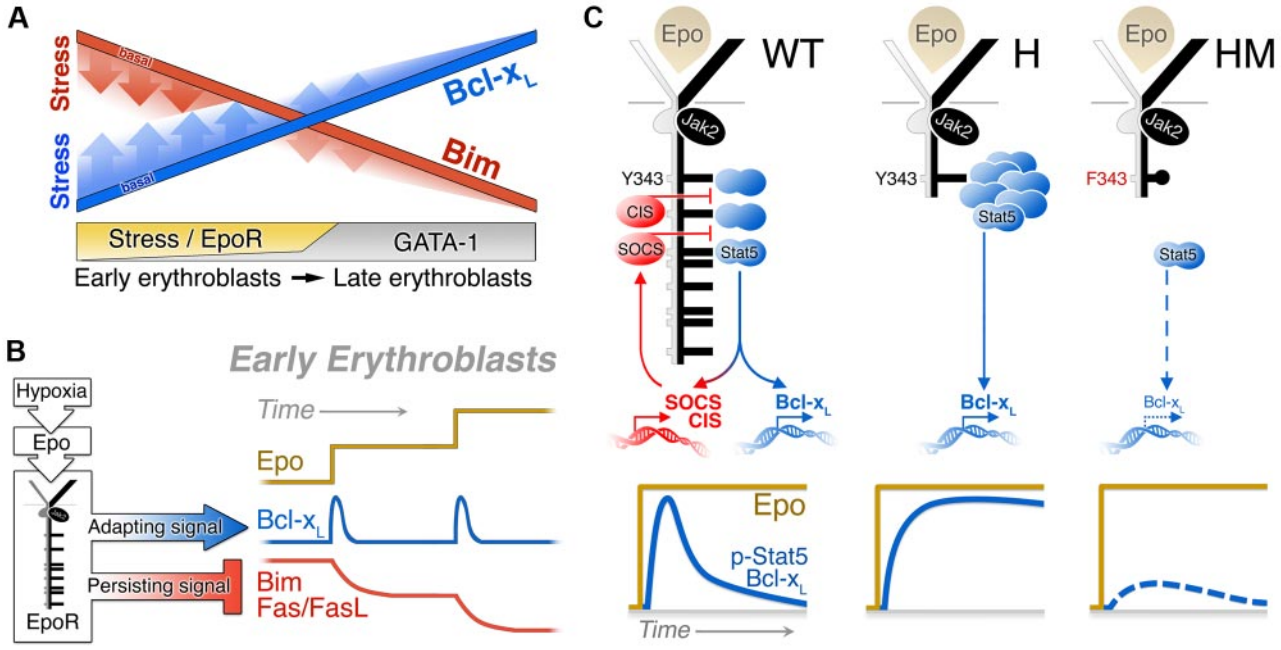

Figure 7. Regulation of Bcl-x_L and Bim expression in erythropoiesis. (A) Model depicting expression of Bcl-x_L (red) and Bim (blue) in the late and early erythroblast compartments, in basal erythropoiesis (solid lines) and during stress (fading shaded area). GATA-1 induces Bcl-x_L and suppresses Bim during erythroid differentiation, with maximal responses achieved in late erythroblasts. The effects of EpoR during stress are superimposed on the basal pattern generated by GATA-1. EpoR signaling operates principally in the early erythroblast compartment, accelerating both Bim suppression and Bcl-x_L induction. (B) Contrasting dynamic stress responses of the Bcl-x_L, Bim and Fas pathways, all driven by the EpoR in the early erythroblast compartment. A sudden increase in stress drives a rapid, but transient, adapting Bcl-x_L response. This response is reactivated with a further change in the stress level, but is insensitive to the absolute level of stress. Bim and Fas suppression in response to stress are slower but persistent and reflects the level of stress. (C) Mechanism of adaptation in the Bcl-x_L response. In wild-type mice, p-Stat5 activates the transcription of negative regulators of Jak2 and Stat5 such as SOCS3, SOCS2, and CIS, which bind the EpoR distal cytoplasmic domain, limiting the duration of both the p-Stat5 and the Bcl-x_L responses. In EpoR-H mice, absence of the distal EpoR domain results in a prolonged response and loss of adaptation. In EpoR-HM mice, both p-Stat5 activation and induction Bcl-x_L are drastically attenuated because of the absence of Stat5 phosphotyrosine docking sites on the EpoR-HM mutant receptor.

In late erythroblasts, Bim, Bcl-x_L, and Fas expression are relatively unaffected by EpoR signaling. Consistent with this, in Stat5$^{-/-}$ embryos and in EpoR-HM mice, where EpoR-Stat5 signaling is deficient, Bcl-x_L in late erythroblasts is only modestly lower.

The finding that EpoR induces Bcl-x_L in early erythroblasts in vivo is consistent with extensive literature showing Bcl-x_L induction in response to EpoR signaling in vitro.[8,13,20-23,27] Our findings, however, also suggest that, after its initial activation, the EpoR-Stat5-Bcl-x_L pathway becomes refractory to high Epo. This property may explain the failure of one report to detect Bcl-x_L induction in BM erythroblasts that were previously subjected to expansion in vitro under prolonged stress-like growth conditions.[50] The same group reported Bcl-x_L induction in response to Epo in subsequent work.[11,51] Importantly, our results show that Stat5-regulated Bcl-x_L expression in vivo varies with differentiation stage, with embryonic day, and with the phase of the stress response. These factors should therefore be considered in the interpretation of Bcl-x_L measurements both in vivo and in vitro.

Adaptation allows functional specialization of the Bcl-x_L response to the acute phase of stress

The acute and chronic phases of the stress response differ in their requirements. At the onset of stress the speed of response is paramount, a property that is unimportant during the chronic maintenance phase. Here we find that Bcl-x_L up-regulation in response to hypoxia is significantly faster than Bim or Fas suppression (Figure 4). In addition, the Bcl-x_L response undergoes rapid adaptation, which makes it insensitive to the prevailing absolute level of stress. However, like other classic sensory adapting mechanisms, it is reactivated as soon as a new change in stress takes place. In this way, the dynamic range of the Bcl-x_L response is extended, allowing a rapid response to changes in stress irrespective of the baseline stress levels.

In addition to Bcl-x_L, other survival pathways, including Bim and Fas suppression, likely contribute to the acute phase of stress. Indeed, Bim is suppressed with fast kinetics in spleen ProE in response to high Epo (Figure 3C); we recently showed that the Fas suppression pathway accelerates the stress response.[19] Maximal Bim and Fas suppression, however, do not occur until 48 to 72 hours from the onset of stress, by which time Bcl-x_L has returned to its baseline value. Therefore, Bcl-x_L likely enhances erythroblast survival during an early phase of stress before the full establishment of the stress response. The EpoR is therefore capable of generating both a persistent signal, giving rise to persistent suppression of Bim and Fas, and a rapidly adapting signal, responsible for the adaptation of the Bcl-x_L response (Figure 7B).

The picture that emerges is of several survival pathways, potentially some as yet to be characterized, with specialization for either the acute or chronic phases of stress, contributing quantitatively to the stress response. The quantitative contribution of both the Bim and Bcl-x_L pathways is in agreement with the current understanding of Bcl-2 family protein interactions, where proapoptotic BH3-only proteins such as Bim are stoichiometrically neutralized by antiapoptotic proteins such as Bcl-x_L.[52] These stoichiometric relationships suggest that both the 4- to 5-fold increase in Bcl-x_L, as well as the 2-fold decrease in Bim, contribute to the survival status of ProE in response to Epo.

Mechanism of adaptation in the Bcl-x_L response

We identified adaptation in the p-Stat5 response in erythroblasts in vivo and suggest this to be the mechanism of adaptation in the Bcl-x_L response. Both p-Stat5 and Bcl-x_L respond similarly to an acute-on-chronic stress stimulus, a response typical of other biologic adapting systems like sensory adaptation or neutrophil chemotaxis. Adaptation of both p-Stat5 and Bcl-x_L depend on the distal domain of the EpoR, a previously documented negative regulatory domain that contains docking sites for the Stat5-induced SOCS family of negative regulators[2] (Figure 7C). Negative feedback is a well-documented mechanism of adaptation in sensory systems.[45,46] Stat5 transcriptionally activates SOCS inhibitors that feed back to limit Jak2 and Stat5 activation.[47] Although well-documented, the precise effect of this pathway on the p-Stat5 signal was not previously investigated. Here we found that in EpoR-H mice that lack this feedback inhibition, peak p-Stat5 signal intensity is not higher than in wild type. However, the duration of the peak is prolonged (Figure 6D). Therefore, p-Stat5–mediated negative feedback is likely responsible for the adaptation of both the p-Stat5 and Bcl-x_L responses.

Implications for myeloproliferative disease mechanisms

The rapid adaptation of the Bcl-x_L response to stress raises the possibility that prolonged periods in which Bcl-x_L is elevated may be harmful. Indeed, persistently elevated levels of Bcl-x_L are characteristic of polycythemia vera and other myeloproliferative syndromes.[28,29,53] High Bcl-x_L was suggested as a cause of Epo-independent erythroid differentiation in polycythemia vera and of the apoptosis resistance of other myeloproliferative syndromes and neoplasms.[28,53,54] Our results, supported by recent reports of SOCS protein inactivation in myeloproliferative disease,[55,56] suggest that impairment of p-Stat5 and Bcl-x_L adaptation may contribute to their prolonged activation. Together, these point to the importance of adaptation in the Bcl-x_L response as a homeostatic and tumor-suppressive mechanism.

Acknowledgments

The authors thank the University of Massachusetts flow cytometry core: Richard Konz, Ted Giehl, Barbara Gosselin, and Yuehua Gu; Dr Volker Haase (Vanderbilt University Medical Center, Nashville, TN) for the ts-VHL$^{-/-}$ mice; Dr Jim Ihle (St Jude Children's Research Hospital, Memphis, TN) for the EpoR-H and EpoR-HM mice; and Dr Lothar Hennighausen (National Institute of Diabetes and Digestive and Kidney Diseases, Bethesda, MD) for the Stat5$^{-/-}$ mice.

This work was funded by National Institutes of Health/National Heart, Lung, and Blood Institute RO1 HL084168. Core resources supported by the Diabetes Endocrinology Research Center grant DK32520 were also used.

Authorship

Contribution: M.K. and E.P. designed and performed research, analyzed and interpreted data, and wrote the manuscript; P.A.P., Y.L., K.H., and D.H. designed and performed research, and analyzed and interpreted data; and M.S. designed research, analyzed and interpreted data, and wrote the manuscript.

Conflict-of-interest disclosure: The authors declare no competing financial interests.

Correspondence: Merav Socolovsky, Department of Pediatrics, Hematology/Oncology Division, and Department of Cancer Biology, University of Massachusetts Medical School, 364 Plantation St, LRB Rm 403, Worcester, MA 01605; e-mail: merav.socolovsky@umassmed.edu.

References

1. Erslev AJ, Caro J. Erythropoietin titers in response to anemia or hypoxia. *Blood Cells.* 1987; 13(1-2):207-216.
2. Lodish HF, Ghaffari S, Socolovsky M, Tong W, Zhang J. Intracellular signaling by the erythropoietin receptor. In: Elliott SG, Foote M, Molineux G, eds. *Erythropoietins, Erythropoietic Factors, and Erythropoiesis: Molecular, Cellular, Preclinical, and Clinical Biology.* Basel, Switzerland: Birkhäuser; 2009:155-174.
3. Koury MJ, Bondurant MC. The molecular mechanism of erythropoietin action. *Eur J Biochem.* 1992;210(3):649-663.
4. Koury MJ, Bondurant MC. Erythropoietin retards DNA breakdown and prevents programmed death in erythroid progenitor cells. *Science.* 1990; 248(4953):378-381.
5. Liu Y, Pop R, Sadegh C, Brugnara C, Haase VH, Socolovsky M. Suppression of Fas-FasL coexpression by erythropoietin mediates erythroblast expansion during the erythropoietic stress response in vivo. *Blood.* 2006;108(1):123-133.
6. Peslak SA, Wenger J, Bemis JC, et al. Sublethal radiation injury uncovers a functional transition during erythroid maturation. *Exp Hematol.* 2011; 39(4):434-445.
7. Chen K, Liu J, Heck S, Chasis JA, An X, Mohandas N. Resolving the distinct stages in erythroid differentiation based on dynamic changes in membrane protein expression during erythropoiesis. *Proc Natl Acad Sci U S A.* 2009;106(41): 17413-17418.
8. Socolovsky M, Fallon AEJ, Wang S, Brugnara C, Lodish HF. Fetal anemia and apoptosis of red cell progenitors in Stat5a−/−5b−/− mice: a direct role for Stat5 in bcl-XL induction. *Cell.* 1999;98: 181-191.
9. Menon MP, Karur V, Bogacheva O, Bogachev O, Cuetara B, Wojchowski DM. Signals for stress erythropoiesis are integrated via an erythropoietin receptor-phosphotyrosine-343-Stat5 axis. *J Clin Invest.* 2006;116(3):683-694.
10. Wood AD, Chen E, Donaldson IJ, et al. ID1 promotes expansion and survival of primary erythroid cells and is a target of JAK2V617F-STAT5 signaling. *Blood.* 2009;114(9):1820-1830.
11. Sathyanarayana P, Dev A, Fang J, et al. EPO receptor circuits for primary erythroblast survival. *Blood.* 2008;111(11):5390-5399.
12. Bouscary D, Pene F, Claessens YE, et al. Critical role for PI 3-kinase in the control of erythropoietin-induced erythroid progenitor proliferation. *Blood.* 2003;101(9):3436-3443.
13. Socolovsky M, Nam H, Fleming MD, Haase VH, Brugnara C, Lodish HF. Ineffective erythropoiesis in Stat5a(−/−)5b(−/−) mice due to decreased survival of early erythroblasts. *Blood.* 2001; 98(12):3261-3273.
14. Halupa A, Bailey ML, Huang K, Iscove NN, Levy DE, Barber DL. A novel role for STAT1 in regulating murine erythropoiesis: deletion of STAT1 results in overall reduction of erythroid progenitors and alters their distribution. *Blood.* 2005;105(2):552-561.
15. Wagner KU, Claudio E, Rucker EB 3rd, et al. Conditional deletion of the Bcl-x gene from erythroid cells results in hemolytic anemia and profound splenomegaly. *Development.* 2000; 127(22):4949-4958.
16. Guihard S, Clay D, Cocault L, et al. The MAPK ERK1 is a negative regulator of the adult steady-state splenic erythropoiesis. *Blood.* 2010;115(18): 3686-3694.
17. Koulnis M, Pop R, Porpiglia E, Shearstone JR, Hidalgo D, Socolovsky M. Identification and analysis of mouse erythroid progenitors using the CD71/Ter119 flow-cytometric assay. *J Vis Exp.* 2011;54:pii:2809.
18. Socolovsky M, Murrell M, Liu Y, Pop R, Porpiglia E, Levchenko A. Negative autoregulation by FAS mediates robust fetal erythropoiesis. *PLoS Biol.* 2007;5(10):e252.
19. Koulnis M, Liu Y, Hallstrom K, Socolovsky M. Negative autoregulation by Fas stabilizes adult erythropoiesis and accelerates its stress response. *PLoS One.* 2011;6(7):e21192.
20. Dolznig H, Grebien F, Deiner EM, et al. Erythroid progenitor renewal versus differentiation: genetic evidence for cell autonomous, essential functions of EpoR, Stat5 and the GR. *Oncogene.* 2006; 25(20):2890-2900.
21. Silva M, Grillot D, Benito A, Richard C, Nunez G, Fernandez-Luna JL. Erythropoietin can promote erythroid progenitor survival by repressing apoptosis through Bcl-XL and Bcl-2. *Blood.* 1996; 88(5):1576-1582.
22. Gregoli PA, Bondurant MC. The roles of bcl-X and apopain in the control of erythropoiesis by erythropoietin. *Blood.* 1997;90(2):630-640.

23. Gregory T, Yu C, Ma A, Orkin SH, Blobel GA, Weiss MJ. GATA-1 and Erythropoietin cooperate to promote erythroid cell survival by regulating bcl-xL expression. *Blood.* 1999;94(1):87-96.
24. Motoyama N, Kimura T, Takahashi T, Watanabe T, Nakano T. bcl-x prevents apoptotic cell death of both primitive and definitive erythrocytes at the end of maturation. *J Exp Med.* 1999;189(11): 1691-1698.
25. Teglund S, McKay C, Schuetz E, et al. Stat5a and Stat5b proteins have essential and nonessential, or redundant, roles in cytokine responses. *Cell.* 1998;93(5):841-850.
26. Schweers RL, Zhang J, Randall MS, et al. NIX is required for programmed mitochondrial clearance during reticulocyte maturation. *Proc Natl Acad Sci U S A.* 2007;104(49):19500-19505.
27. Rhodes MM, Kopsombut P, Bondurant MC, Price JO, Koury MJ. Bcl-x(L) prevents apoptosis of late-stage erythroblasts but does not mediate the anti-apoptotic effect of erythropoietin. *Blood.* 2005;106(5):1857-1863.
28. Garcon L, Rivat C, James C, et al. Constitutive activation of STAT5 and Bcl-xL overexpression can induce endogenous erythroid colony formation in human primary cells. *Blood.* 2006;108(5): 1551-1554.
29. Silva M, Richard C, Benito A, Sanz C, Olalla I, Fernandez-Luna JL. Expression of Bcl-x in erythroid precursors from patients with polycythemia vera. *N Engl J Med.* 1998;338(9):564-571.
30. Green DR. Life, death, BH3 profiles, and the salmon mousse. *Cancer Cell.* 2007;12(2):97-99.
31. Kuribara R, Honda H, Matsui H, et al. Roles of Bim in apoptosis of normal and Bcr-Abl-expressing hematopoietic progenitors. *Mol Cell Biol.* 2004;24(14):6172-6183.
32. Shinjyo T, Kuribara R, Inukai T, et al. Downregulation of Bim, a proapoptotic relative of Bcl-2, is a pivotal step in cytokine-initiated survival signaling in murine hematopoietic progenitors. *Mol Cell Biol.* 2001;21(3):854-864.
33. Abutin RM, Chen J, Lung TK, Lloyd JA, Sawyer ST, Harada H. Erythropoietin-induced phosphorylation/degradation of BIM contributes to survival of erythroid cells. *Exp Hematol.* 2009; 37(2):151-158.
34. Maeda T, Ito K, Merghoub T, et al. LRF is an essential downstream target of GATA1 in erythroid development and regulates BIM-dependent apoptosis. *Dev Cell.* 2009;17(4):527-540.
35. Zang H, Sato K, Nakajima H, McKay C, Ney PA, Ihle JN. The distal region and receptor tyrosines of the Epo receptor are nonessential for in vivo erythropoiesis. *EMBO J.* 2001;20(12):3156-3166.
36. Pop R, Shearstone JR, Shen Q, et al. A key commitment step in erythropoiesis is synchronized with the cell cycle clock through mutual inhibition between PU.1 and S-phase progression. *PLoS Biol.* 2010;8(9):e1000484.
37. Cui Y, Riedlinger G, Miyoshi K, et al. Inactivation of Stat5 in mouse mammary epithelium during pregnancy reveals distinct functions in cell proliferation, survival, and differentiation. *Mol Cell Biol.* 2004;24(18):8037-8047.
38. Zhu BM, McLaughlin SK, Na R, et al. Hematopoietic-specific Stat5-null mice display microcytic hypochromic anemia associated with reduced transferrin receptor gene expression. *Blood.* 2008;112(5):2071-2080.
39. Kerenyi MA, Grebien F, Gehart H, et al. Stat5 regulates cellular iron uptake of erythroid cells via IRP-2 and TfR-1. *Blood.* 2008;112(9):3878-3888.
40. Pugh LG. Blood volume and haemoglobin concentration at altitudes above 18,000 ft. (5500 M). *J Physiol.* 1964;170:344-354.
41. Schmidt W. Effects of intermittent exposure to high altitude on blood volume and erythropoietic activity. *High Alt Med Biol.* 2002;3(2):167-176.
42. Yang B, Kirby S, Lewis J, Detloff PJ, Maeda N, Smithies O. A mouse model for beta 0-thalassemia. *Proc Natl Acad Sci U S A.* 1995;92(25): 11608-11612.
43. Haase VH, Glickman JN, Socolovsky M, Jaenisch R. Vascular tumors in livers with targeted inactivation of the von Hippel-Lindau tumor suppressor. *Proc Natl Acad Sci U S A.* 2001;98:1583-1588.
44. Tyson JJ, Chen KC, Novak B. Sniffers, buzzers, toggles and blinkers: dynamics of regulatory and signaling pathways in the cell. *Curr Opin Cell Biol.* 2003;15(2):221-231.
45. Yi TM, Huang Y, Simon MI, Doyle J. Robust perfect adaptation in bacterial chemotaxis through integral feedback control. *Proc Natl Acad Sci U S A.* 2000;97(9):4649-4653.
46. Kuhara A, Inada H, Katsura I, Mori I. Negative regulation and gain control of sensory neurons by the C. elegans calcineurin TAX-6. *Neuron.* 2002; 33(5):751-763.
47. Wormald S, Hilton DJ. Inhibitors of cytokine signal transduction. *J Biol Chem.* 2004;279(2):821-824.
48. Klingmuller U, Bergelson S, Hsiao JG, Lodish HF. Multiple tyrosine residues in the cytosolic domain of the erythropoietin receptor promote activation of STAT5. *Proc Natl Acad Sci U S A.* 1996;93(16): 8324-8328.
49. Socolovsky M. Molecular insights into stress erythropoiesis. *Curr Opin Hematol.* 2007;14(3): 215-224.
50. Menon MP, Fang J, Wojchowski DM. Core erythropoietin receptor signals for late erythroblast development. *Blood.* 2006;107(7):2662-2672.
51. Dev A, Fang J, Sathyanarayana P, Pradeep A, Emerson C, Wojchowski DM. During EPO or anemia challenge, erythroid progenitor cells transit through a selectively expandable proerythroblast pool. *Blood.* 2010;116(24):5334-5346.
52. Chipuk JE, Green DR. How do BCL-2 proteins induce mitochondrial outer membrane permeabilization? *Trends Cell Biol.* 2008;18(4):157-164.
53. Hsieh PP, Olsen RJ, O'Malley DP, et al. The role of Janus kinase 2 V617F mutation in extramedullary hematopoiesis of the spleen in neoplastic myeloid disorders. *Mod Pathol.* 2007;20(9):929-935.
54. Diaz T, Navarro A, Ferrer G, et al. Lestaurtinib inhibition of the Jak/STAT signaling pathway in Hodgkin lymphoma inhibits proliferation and induces apoptosis. *PLoS ONE.* 2011;6(4):e18856.
55. Capello D, Deambrogi C, Rossi D, et al. Epigenetic inactivation of suppressors of cytokine signalling in Philadelphia-negative chronic myeloproliferative disorders. *Br J Haematol.* 2008; 141(4):504-511.
56. Fernandez-Mercado M, Cebrian V, Euba B, et al. Methylation status of SOCS1 and SOCS3 in BCR-ABL negative and JAK2V617F negative chronic myeloproliferative neoplasms. *Leuk Res.* 2008;32(10):1638-1640.